Hindawi
International Journal of Photoenergy
Volume 2022, Article ID 7761031, 14 pages
https://doi.org/10.1155/2022/7761031

Research Article

Nonlinear Observation and Control of Series Active Power Filters in the Presence of Voltage Sags

Younes Abouelmahjoub,[1] **Said El Beid**,[2] **Hassan Abouobaida**,[1] **and Abdelkhalek Chellakhi**[1]

[1]*LabSIPE, National School of Applied Sciences, Chouaib Doukkali University, El Jadida 24000, Morocco*
[2]*CISIEV Team, Cadi Ayyad University, Marrakech 40160, Morocco*

Correspondence should be addressed to Younes Abouelmahjoub; abouelmahjoub.y@ucd.ac.ma

Received 2 August 2021; Revised 31 December 2021; Accepted 8 January 2022; Published 8 February 2022

Academic Editor: Mark van Der Auweraer

This study addresses the problem of controlling series active power filters for voltage sag compensation. Indeed, we can control this kind of filter to generate a voltage series that compensates the grid voltage sag in order to protect the sensitive loads against this perturbation. This study is aimed at seeking a control strategy that meets the main control objective, which is the compensation of grid voltage sags and this by considering the following technical constraints: (i) the nonlinearity of the system dynamics, (ii) the high dimension of the system model, and (iii) the inaccessibility of some system variables to measurements. To meet the main control objective, we propose a nonlinear controller that is designed based on the system nonlinear model, using the backstepping technique. This controller involves a nonlinear regulator and a grid observer. The former copes with the compensation issue. The observer provides online the grid voltage estimations. In addition to a theoretical analysis of the control system, the performances of the proposed controller are evaluated by simulation using MATLAB/Simulink.

1. Introduction

The voltage wave of the power grid can be affected by voltage sag, which is a sudden decrease in the magnitude of the electrical voltage below a lower threshold of the nominal range. It is characterized by its duration which can range from 10 ms to 3 min and by its depth between 10% and 90% of the nominal voltage. The consequences of voltage sags can be extremely costly (including the incorrect operation of some sensitive loads, disruption or stoppage of production, loss of computer data, stalling of motors, and extinction of lamps). Series active power filters represent an appropriate solution to protect the sensitive loads (such as switching power supplies, motor drivers, and medical equipment) against voltage sags [1, 2].

In this study, we are interested in single-phase half-bridge series active power filters connected between the power grid and the sensitive loads (e.g., consumer electronics, variable frequency motor drives, computer numerical control equipment, and automated systems and processes). Half-bridge topology of the inverter [3, 4] enjoys several features compared to full-bridge topology [5–8]. The main features are the following: (i) a reduced number of power electronic components which entails lower cost, (ii) a reduced number of switches which results in less control functions increasing system reliability, and (iii) a reduced switching power loss of the inverter. In the literature, several control strategies have been proposed for series active power filters (e.g., [3, 6–14]) to improve the voltage quality at terminals of sensitive loads. Among them, we find the linear controls [6–9]. With these control approaches in [6–9], the optimal performances are not guaranteed in a wide variation range because of the presence of controlled system nonlinearity. To overcome this handicap, nonlinear controls based

on accurate nonlinear models of the controlled system have been proposed, e.g., sliding mode control for the series active power filter in [3, 10] and backstepping control in [11]; in [12], a passivity control is applied for the series active power filter, and reference [13] introduced a modified recursive least square (RLS) algorithm to cope with the multioutput systems (MO) and applied this MO-RLS to the symmetrical component estimation. Consequently, the proposed control methodology combines the advantages of both the RLS algorithm and the symmetrical component method to come out with a flexible algorithm for sag compensation. In [14], the control strategy of the series active power filter is achieved through the synchronous reference frame theory for the generation of the reference voltage which is compared with constant voltage for pulse generation using hysteresis band PWM.

In light of the precedent description, firstly, we note that the researchers often use a control strategy based on the instantaneous power method (e.g. [1, 15]) to cope with the compensation problem. On the other hand, all previous controllers (e.g. [3, 6–12]) are simple because they are seen to be based on the assumption that all system variables are accessible to measurements, including the grid voltage. This assumption is not satisfied in practical applications. Moreover, another limitation in the previous works is that no theoretical analysis of the stability in closed-loop system is established.

Compared to works [2, 10–13], which also presented a nonlinear controller for series active power filters, the present nonlinear controller enjoys several appealing features as follows:

(1) The present controller is developed for the half-bridge converter which features fewer switches and a smaller number of gate drivers, compared to the full-bridge converter used in [2, 10–13]. As a result, the present nonlinear controller is simpler to implement because it involves fewer control signals to generate and apply

(2) The controller design proposed in [2, 10–13] is based on the assumption that the grid impedance was supposed to be zero [2, 10–13] which entails an approximate system model used in the control design. Furthermore, all electrical signals (voltage and current), including the grid voltage, were assumed to be accessible to measurements in [2, 10–12], but not the case here. Also, the present controller is simpler because it does not necessitate sensors for the measurement of the grid voltage

In the present paper, we study the problem of controlling a single-phase half-bridge series active power filter operating in the presence of sensitive loads. This study consists of controlling the series active power filter to compensate for grid voltage sags while taking into account the following technical constraints: (i) the nonlinearity of the system dynamics, (ii) the high dimension of the system model, and (iii) the inaccessibility of some system variables to measurements. To carry out this study, we seek a new control strategy while meeting the following requirements:

(i) Development of a more accurate model for the series active power filter by considering the parameters of the grid impedance

(ii) Observation of some system variables which are supposed to be not accessible to measurements

(iii) Satisfactory compensation of the power grid voltage sags in order to protect the sensitive load

To achieve the above requirements, we build up a new nonlinear controller based on a more accurate system model to meet the voltage sag compensation. A major feature of the new controller is that there is no subject to the precedent limitations, i.e., the grid internal impedance is not neglected, and not all system internal states are assumed to be accessible to measurements. To this end, this controller includes a nonlinear observer providing online estimates of the grid voltage based only on the grid current measurements. It also includes a nonlinear voltage regulator designed using the backstepping technique to compensate for the voltage sags. By using various tools such as Lyapunov stability and averaging theory, a rigorous theoretical analysis on the stability of the control system in a closed loop is developed to show that the proposed controller achieves the main objective for which it was designed. Several simulation results in MATLAB/Simulink completely show additional robustness features and also show the supremacy of the proposed nonlinear controller, over linear model-based controllers.

A prefatory version of this paper has been presented at the conference [4]. This journal paper differs from the conference version [4] in which (i) it proposes a nonlinear controller (whereas the conference paper assumed all signals to be accessible to measurements); accordingly, the present controller (includes a nonlinear observer) differs from the one (no observer) in the conference paper; (ii) it includes all proofs whereas these were incomplete in the conference paper [4]; and (iii) it contains more simulation results.

The paper is organized as follows: the system modeling is presented in Section 2, the nonlinear controller design including the nonlinear observer is described in Section 3, the stability analysis of the control system is described in Section 4, and the performances of the nonlinear controller including the grid observer are checked by simulation in Section 5.

2. System Modeling

The topology of the series active power filter (SAPF) under study is shown in Figure 1. It is composed of (i) a half-bridge converter involving two switches based on an IGBT diode, (ii) two identical capacitors C_d placed at the DC bus of the converter, (iii) filtering impedance (R_f, L_f, C_f), and (iv) a current transformer.

The active power filter is connected in series with the perturbed power grid. This grid supplies a sensitive load. The role of this filter is the compensation of grid voltage

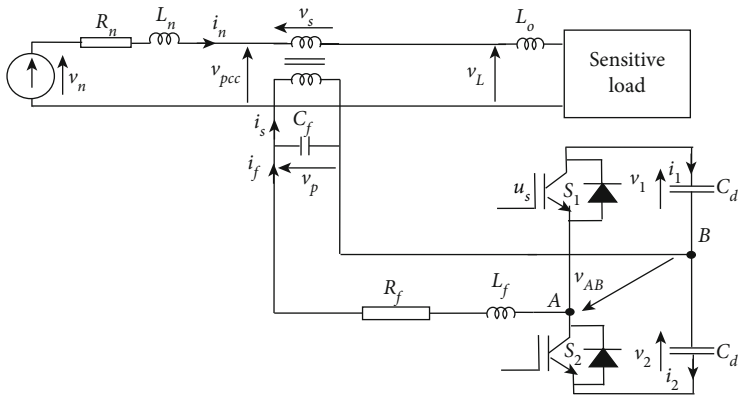

Figure 1: Single-phase half-bridge series active power filter operating with a sensitive load.

perturbation in order to protect the sensitive load. The internal model of the power grid includes a voltage v_n in series with an internal impedance formed by a resistor R_n and an inductor L_n. Notice that the power grid voltage v_n is inaccessible to measurements; it is given by

$$v_n(t) = E_n \sin(\omega_n t). \tag{1}$$

The half-bridge converter operates under the technique of pulse width modulation (PWM) (e.g., [4, 16–18]).

By applying Kirchhoff's laws to the system of Figure 1, the instantaneous model of the half-bridge series active power filter is as follows:

$$L_n \frac{di_n}{dt} + R_n i_n = v_n - v_{\text{PCC}}, \tag{2a}$$

$$L_f \frac{di_f}{dt} + R_f i_f = v_{AB} - v_p, \tag{2b}$$

$$C_f \frac{dv_p}{dt} = i_f - i_s, \tag{2c}$$

$$C_d \frac{dv_1}{dt} = i_1, \tag{2d}$$

$$C_d \frac{dv_2}{dt} = i_2. \tag{2e}$$

The following quantities v_{AB}, i_1, i_2, v_p, i_s, and v_{PCC} undergo the following equations:

$$v_{AB} = \frac{(1+\mu_s)v_1}{2} - \frac{(1-\mu_s)v_2}{2}, \tag{3a}$$

$$i_1 = -\frac{(1+\mu_s)i_f}{2}, \tag{3b}$$

$$i_2 = \frac{(1+\mu_s)i_f}{2}, \tag{3c}$$

$$v_p = \frac{v_s}{m_s}, \tag{3d}$$

$$i_s = -m_s i_n, \tag{3e}$$

$$v_{\text{PCC}} = v_s + v_L, \tag{3f}$$

where the switching function μ_s is defined as follows:

$$\mu_s = \begin{cases} +1 \text{ if } S_1 \text{ is ON and } S_2 \text{ is } \textbf{\textit{OFF}} \\ -1 \text{ if } S_1 \text{ is OFF and } S_2 \text{ is } \textbf{\textit{ON}} \end{cases} \tag{4}$$

Substituting (3a)–(3f) in (2a)–(2e), we get the following instantaneous model:

$$L_n \frac{di_n}{dt} + R_n i_n = v_n - v_s - v_L, \tag{5a}$$

$$L_f \frac{di_f}{dt} + R_f i_f = \mu_s \frac{v_o}{2} + \frac{v_d}{2} - \frac{v_s}{m_s}, \tag{5b}$$

$$C_f \frac{dv_s}{dt} = m_s i_f + m_s^2 i_n, \tag{5c}$$

$$C_d \frac{dv_o}{dt} = -\mu_s i_f, \tag{5d}$$

$$C_d \frac{dv_d}{dt} = -i_f, \tag{5e}$$

with $v_o = v_1 + v_2$ and $v_d = v_1 - v_2$.

Equation (5a) is completed by the model of the voltage $v_n(t)$ of the electrical grid given by

$$\frac{d^2 v_n}{dt^2} = -\omega_n^2 v_n. \tag{5f}$$

The above-obtained model (5a)–(5f) cannot be used to design a controller to pilot the system under study due to the binary nature of the control input μ_s. To overcome this difficulty, the different signals of the instantaneous model are replaced by their average values over the cutting period [4, 17, 18]. Doing so, we obtain the following average model, where the notations are defined in Table 1:

$$\dot{x}_1 = \frac{1}{L_n}(-R_n x_1 + x_2 - x_4 - v_L), \tag{6a}$$

Table 1: State variables.

State variables and parameters	Definition	Observation
x_1	Averaged i_n	Accessible to measurements
x_2	Averaged v_n	Not accessible to measurements
x_3	Averaged $\dot{v}_n$	Not accessible to measurements
x_4	Averaged v_s	Accessible to measurements
x_5	Averaged i_f	Accessible to measurements
x_6	Averaged v_o	Accessible to measurements
x_7	Averaged v_d	Accessible to measurements

$$\dot{x}_2 = x_3, \tag{6b}$$

$$\dot{x}_3 = -\omega_n^2 x_2, \tag{6c}$$

$$\dot{x}_4 = \frac{1}{C_f}\left(m_s^2 x_1 + m_s x_5\right), \tag{6d}$$

$$\dot{x}_5 = \frac{1}{L_f}\left(-\frac{x_4}{m_s} - R_f x_5 + u_s\,\frac{x_6}{2} + \frac{x_7}{2}\right), \tag{6e}$$

$$\dot{x}_6 = -\frac{u_s x_5}{C_d}, \tag{6f}$$

$$\dot{x}_7 = -\frac{x_5}{C_d}. \tag{6g}$$

The average models (6a)–(6g) are nonlinear and their control input is u_s, which represents the average value of the binary signal μ_s, which is continuously varying between −1 and 1.

3. Control Strategy

We seek the achievement of the following main objective:

(i) Compensation of the grid voltage sags in order to protect the sensitive load

A significant and outstanding contribution of this present study is the design of a nonlinear controller for the single-phase series active power filter by adopting the half-bridge topology and taking into account in the present study that the grid impedance is not supposed to be negligible, unlike previous works. Indeed, in most previous works (e.g., [2, 3, 9–11, 13, 14]), the grid internal impedance is supposed to be zero. In others (e.g., [5–8, 15, 19]), the grid internal impedance is not supposed to be zero but all electrical quantities are accessible to measurements, including the grid voltage. Presently, the grid impedance (R_n, L_n) is not zero. This entails that the grid voltage v_n cannot be assumed to be accessible to measurements. This above difficulty is coped with by augmenting the nonlinear controller with a nonlinear observer providing online estimates of the grid voltage based only on the measurements of the grid current i_n. The proposed nonlinear controller is described in Figure 2; it forces the series active power filter to compensate for the grid voltage sags.

3.1. Grid Observer Design. In practice, only the voltage v_{PCC} at PCC should be assumed to be accessible to measurements (see Figure 1). As a result, the power grid voltage v_n is inaccessible to measurements. To surmount this difficulty, we will propose a high-gain observer as in [20] to estimate the state variables not accessible to measurements x_2 and x_3. To this end, we use the following state representation obtained from the model (6a)–(6c) of the power grid:

$$\begin{aligned} \dot{x}_n &= A\,x_n + B, \\ y &= C\,x_n, \end{aligned} \tag{7a}$$

with

$$\begin{aligned} x_n &= \begin{pmatrix} x_1 \\ x_2 \\ x_3 \end{pmatrix}, \\ A &= \begin{pmatrix} -\dfrac{R_n}{L_n} & \dfrac{1}{L_n} & 0 \\ 0 & 0 & 1 \\ 0 & -\omega_n^2 & 0 \end{pmatrix}, \\ B &= \begin{pmatrix} -\dfrac{x_4}{L_n} - \dfrac{v_L}{L_n} \\ 0 \\ 0 \end{pmatrix}, \\ C &= \begin{pmatrix} 1 \\ 0 \\ 0 \end{pmatrix}^T, \end{aligned} \tag{8}$$

where x_n is the state vector, y denotes the system output, and the matrices A, B, and C are known; notice that the pair (A, C) is observable.

Based on the measurements of the grid current, the high-gain observer proposed is as follows:

$$\dot{\hat{x}}_n = A\,\hat{x}_n + B + K(y - C\,\hat{x}_n), \tag{9a}$$

$$\hat{y} = C\,\hat{x}_n, \tag{9b}$$

$(k_1\ k_2\ k_3)^T$ is the gain vector.

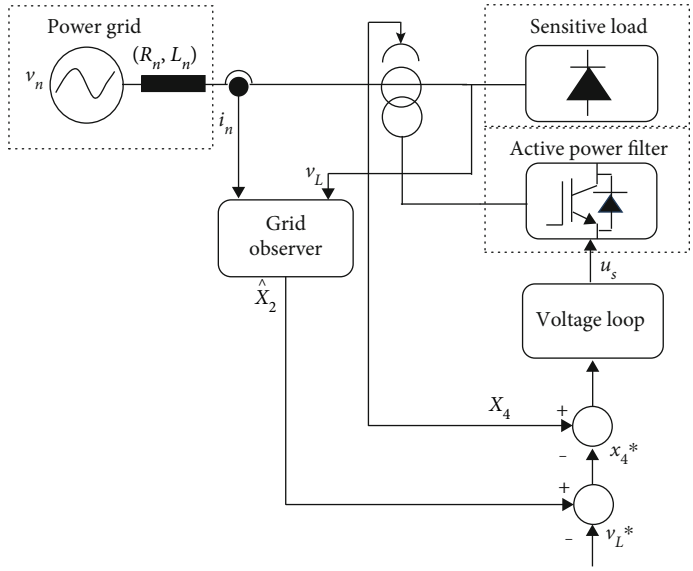

Figure 2: Grid observer and nonlinear controller associated to the series active power filter.

To analyze the convergence of the above observer (9a) and (9b), we introduce the following observation error:

$$\tilde{x}_n = x_n - \hat{x}_n. \tag{10}$$

It is easily checked, by using expressions (9a) and (9b) and (10), that the dynamics of observation error (10) is given as follows:

$$\dot{\tilde{x}}_n = (A - KC)\tilde{x}_n, \tag{11}$$

with

$$A_o = (A - KC) = \begin{pmatrix} -\left(\dfrac{R_n}{L_n} + k_1\right) & \dfrac{1}{L_n} & 0 \\ -k_2 & 0 & 1 \\ -k_3 & -\omega_n^2 & 0 \end{pmatrix}. \tag{12}$$

The gain vector $K = (\,k_1 \quad k_2 \quad k_3\,)^T$ is chosen so that the matrix $A_o = A - KC$ is Hurwitz. It is possible to check by applying the Routh-Hurwitz that the matrix $A_o = A - KC$ is Hurwitz if the gain vector components satisfy the following conditions:

$$\frac{R_n}{L_n} + k_1 > 0, \tag{13}$$

$$\frac{R_n}{L_n} + k_1 > \frac{k_3}{k_2}, \tag{14}$$

$$\frac{R_n}{L_n} + k_1 > -\frac{k_3}{L_n\omega_n^2}. \tag{15}$$

To analyze the convergence properties of the above observer (9a) and (9b), we consider the following Lyapunov function candidate associated with the observation error equation (11):

$$V_{obs} = \frac{1}{2}\tilde{x}_n^T P \tilde{x}_n. \tag{16}$$

The stability results of observer are summarized in the next proposition.

Proposition 1. *Under condition (13), linear system (11) is globally exponentially stable with respect to Lyapunov function (16). Specifically, the following equality holds:*

$$\dot{V}_{obs} = -\frac{1}{2}\tilde{x}_n^T \tilde{x}_n. \tag{17}$$

Doing so, observation error (10) converges exponentially to zero. The estimate $\hat{x}_n$ converges exponentially to its true value x_n. The proof of this proposition is accomplished later.

3.2. Voltage Loop Regulator Design. The control objective of the series active power filter under study is as follows: to protect the sensitive load from the grid voltage sags, the waveform of load voltage v_L should be sinusoidal as follows:

$$v_L^* = E_n \ \sin(\omega_n t). \tag{18}$$

To achieve the above objective, the control requires that the voltage x_4 generated by the series active power filter should follow the best as possible its reference x_4^* defined by

$$x_4^* = \hat{x}_2 - v_L^*. \tag{19}$$

To force the voltage x_4 generated by the series active power filter to track its reference x_4^*, a nonlinear regulator is synthesized by applying the backstepping method (e.g., [18, 21]), which is carried in two steps.

Step 1. Stabilization of the subsystem $(e_1, \tilde{x}_n)$.

To cope with the compensation issue, we introduce the tracking error on the filter voltage x_4:

$$e_1 = x_4 - x_4^*. \tag{20}$$

Using (6d), the dynamics of the tracking error e_1 is given by

$$\dot{e}_1 = \frac{1}{C_f}\left(m_s x_5 + m_s^2 x_1\right) - \dot{x}_4^*. \tag{21}$$

Also using (19) and (9a), the dynamics of the filter voltage reference x_4^* is demonstrated as follows:

$$\dot{x}_4^* = \left(\widehat{x}_3 + k_2\tilde{x}_1\right) - \dot{v}_L^*. \tag{22}$$

The stabilization problem of the error system described by (11) and (21) is solved by considering the following Lyapunov function candidate:

$$V_1 = V_{sys} + V_{obs} = \frac{1}{2}e_1^2 + \frac{1}{2}\tilde{x}_n^T P \tilde{x}_n. \tag{23}$$

The time derivative of (23) is given by

$$\dot{V}_1 = e_1\dot{e}_1 + \frac{1}{2}\left(\dot{\tilde{x}}_n^T P\tilde{x}_n + \tilde{x}_n^T P\dot{\tilde{x}}_n\right) = e_1\dot{e}_1 + \frac{1}{2}\tilde{x}_n^T\left(A_o^T P + PA_o\right)\tilde{x}_n, \tag{24}$$

where P is a symmetric defined positive matrix; it is chosen to satisfy the Lyapunov equation: $A_o^T P + PA_o = -I$; this choice implies that the dynamics of the Lyapunov function candidate (24) becomes:

$$\dot{V}_1 = e_1\dot{e}_1 - \frac{1}{2}\tilde{x}_n^T\tilde{x}_n. \tag{25}$$

Also, replacing (6d) and (22) in (25), we obtain the following dynamics of the Lyapunov function candidate:

$$\dot{V}_1 = e_1\left(\frac{m_s x_5}{C_f} + \frac{m_s^2 x_1}{C_f} - \widehat{x}_3 - k_2\tilde{x}_1 + \dot{v}_L^*\right) - \frac{1}{2}\tilde{x}_n^T\tilde{x}_n. \tag{26}$$

If we consider that $m_s x_5/C_f$ is the virtual control, its desired value σ is defined by

$$\sigma = -c_1 e_1 - \frac{m_s^2 x_1}{C_f} + \widehat{x}_3 + k_2\tilde{x}_1 - \dot{v}_L^*. \tag{27}$$

σ is namely a suitable stabilizing function and c_1 is a positive design parameter.

In fact, with this choice in (27), equation (26) is reduced to

$$\dot{V}_1 = -c_1 e_1^2 - \frac{1}{2}\tilde{x}_n^T\tilde{x}_n. \tag{28}$$

As $m_s x_5/C_f$ is not the actual control variable, a new variable error e_2 between the virtual control and its desired value σ is defined as follows:

$$e_2 = \frac{m_s x_5}{C_f} - \sigma. \tag{29}$$

By deferring (29) in (21), while using (27), it comes

$$\dot{e}_1 = -c_1 e_1 + e_2. \tag{30}$$

Also, the derivative of Lyapunov function candidate (25) becomes

$$\dot{V}_1 = -c_1 e_1^2 + e_1 e_2 - \frac{1}{2}\tilde{x}_n^T\tilde{x}_n. \tag{31}$$

End of step 1.

Step 2. Stabilization of the subsystem $(e_1, \tilde{x}_n, e_2)$.

To achieve the above objective, the controller forces the errors (e_1, e_2) to converge to zero; one needs the dynamics of e_2. Indeed, we derive (29) by using (27) and (6e) and we obtain

$$\dot{e}_2 = \left(\frac{m_s}{C_f L_f}\left(-\frac{x_4}{m_s} - R_f x_5 + u_s\frac{x_6}{2} + \frac{x_7}{2}\right)\right) - \left(-c_1\dot{e}_1 - \frac{m_s^2\dot{x}_1}{C_f} + \left(\dot{\widehat{x}}_3 + k_2\dot{\tilde{x}}_1\right) - \ddot{v}_L^*\right). \tag{32}$$

Table 2: Parameter system.

Parameters	Symbol	Values
Power grid	E_n	$220\sqrt{2}$ V/50 Hz
	R_n	50 m Ω
	L_n	0.5 mH
Single-phase half-bridge series active power filter	R_f	80 mΩ
	L_f	3 mH
	C_f	1200 μF
DC bus	C_d	9000 μF
Sensitive load	R	20 Ω
	L	500 mH
	L_o	5 mH

Table 3: Parameters of the grid observer and controller.

Parameters	Symbol	Values
Grid observer	k_1	10^4
	k_2	10^5
	k_3	10^5
Voltage regulator	c_1	3000 s^{-1}
	c_2	6000 s^{-1}

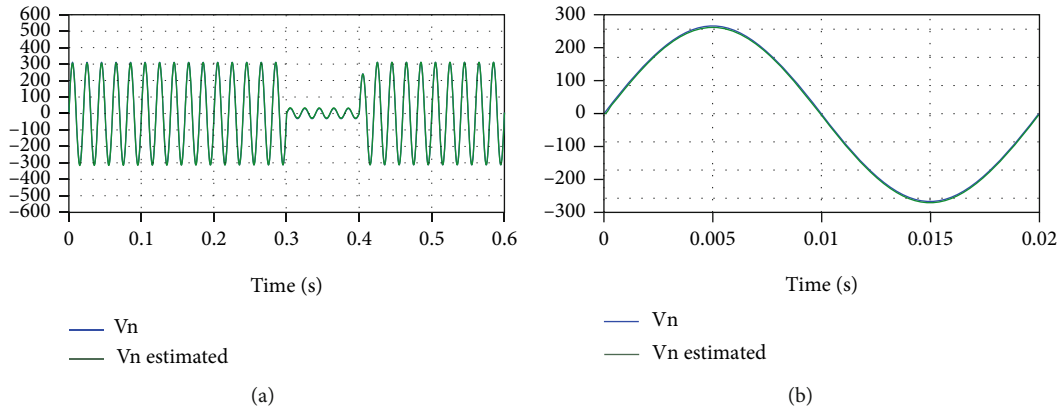

Figure 3: (a) Grid voltage x_2 and its estimated $\hat{x}_2$. (b) Zoom on these signals.

The actual control variable, namely, u_s, appears for the first time in (32). Let us consider the following Lyapunov candidate function.

$$V_2 = V_1 + \frac{1}{2}e_2^2. \tag{33}$$

Using (31), the dynamics of V_2 is given by

$$\dot{V}_2 = -c_1 e_1^2 + e_2(e_1 + \dot{e}_2) - \frac{1}{2}\tilde{x}_n^T \tilde{x}_n. \tag{34}$$

This shows that, for the (e_1, e_2) system to be globally asymptotically stable, it is sufficient to choose the control input u_s so that $\dot{V}_2 = -c_1 e_1^2 - c_2 e_2^2 - (1/2)\tilde{x}_n^T \tilde{x}_n$ which, considering equation (34), amounts to ensuring that

$$\dot{e}_2 = -c_2 e_2 - e_1, \tag{35}$$

where c_2 is a positive design parameter.

From equations (32) and (35), we deduce the following backstepping control law u_s:

$$u_s = \left(\frac{2R_f x_5}{x_6} - \frac{x_7}{x_6} + \frac{2x_4}{m_s x_6} + \frac{2C_f L_f}{m_s x_6} \cdot \left(-e_1 - c_2 e_2 + \left(-c_1 \dot{e}_1 - \frac{m_s^2 \dot{x}_1}{C_f} + \dot{\hat{x}}_3 + k_2 \dot{\tilde{x}}_1 - \ddot{v}_L^*\right)\right)\right). \tag{36}$$

The above results are stated in the following proposition:

Proposition 2. *Consider the series active power filter of Figure 1 described by its average models (6a)–(6g) with the control law (36); then, the closed-loop system is globally asymptotically stable. Specifically, its dynamics is described in the coordinates $(e_1, e_2, \tilde{x}_n)$ by equations (37a) and (37b):*

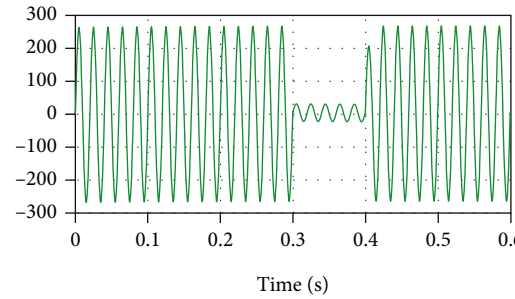

Figure 4: A sag in the estimated signal of grid voltage $\hat{x}_2$.

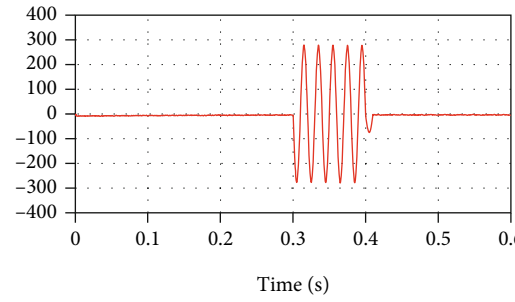

Figure 5: Compensation voltage v_s.

$$\begin{pmatrix} \dot{e}_1 \\ \dot{e}_2 \end{pmatrix} = \begin{pmatrix} -c_1 & 1 \\ -1 & -c_2 \end{pmatrix} \begin{pmatrix} e_1 \\ e_2 \end{pmatrix} \text{ putting } A_1 = \begin{pmatrix} -c_1 & 1 \\ -1 & -c_2 \end{pmatrix}, \tag{37a}$$

$$\dot{\tilde{x}}_n = A_o \tilde{x}_n. \tag{37b}$$

Systems (37a) and (37b) are globally asymptotically stable because matrix A_o is Hurwitz.

Remark 3. Although the backstepping control law (36) involves a division by the DC bus voltage x_6, there is no risk of singularity because in practice, the DC bus voltage remains all the time positive. Otherwise, the power converter cannot work.

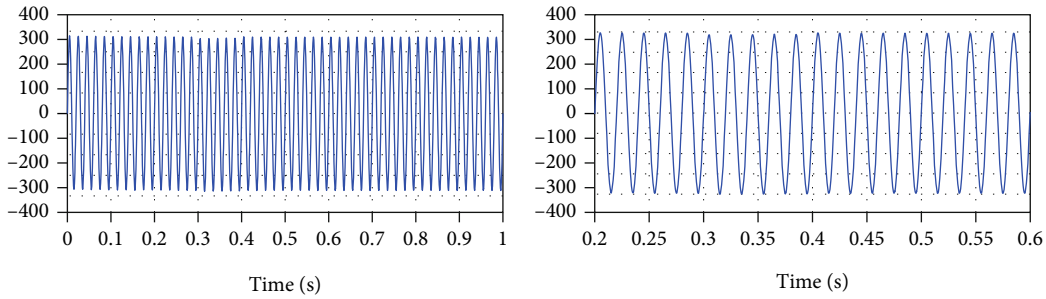

Figure 6: (a) Voltage v_L at the terminals of sensitive load after compensation. (b) Zoom of this signal.

4. Stability Analysis of the Control System

In the following theorem, we need the following notations to formulate the results of stability analysis.

$$\varepsilon = \frac{1}{\omega_n}, \quad a_0 = 1 + c_1 c_2, \quad a_1 = c_1 + c_2. \tag{38}$$

Theorem 4 (main result). *Consider the series active power filter described in Figure 1, represented by its average models (6a)–(6g), where the state variables (x_2, x_3) are inaccessible to measurements. The closed-loop system formed by the series active power filter and the control system consist of the following:*

(i) Grid observers (9a) and (9b), with the gain vector $K = (k_1 \quad k_2 \quad k_3)^T$ which are selected so that the matrix $A_o = A - KC$ is Hurwitz

(ii) The control law (36), where (c_1, c_2) are any positive design parameters

Then, the closed-loop control system has the following properties:

(1) The tracking errors (e_1, e_2) vanish exponentially fast

(2) By associating equations (11), (30), and (35), we defined the augmented state vector $Z(t) = (z_1 \quad z_2 \quad z_3 \quad z_4 \quad z_5)^T = (e_1 \quad e_2 \quad \tilde{x}_1 \quad \tilde{x}_2 \quad \tilde{x}_3)^T$; this latter obeys the following state equation:

$$\dot{Z} = f(t, Z), \tag{39a}$$

where

$$f(t,z) = \begin{pmatrix} -c_1 z_1 + z_2 \\ -z_1 - c_2 z_2 \\ -\left(\frac{R_n}{L_n} + k_1\right) z_3 + \frac{z_4}{L_n} \\ -k_2 z_3 + z_5 \\ -k_3 z_3 - \omega_n^2 z_4 \end{pmatrix} \tag{39b}$$

(3) If the design parameters (c_1, c_2) of control are chosen so that the following inequalities

$$a_0 = 1 + c_1 c_2 > 0, \tag{40}$$

$$a_1 = c_1 + c_2 > 0 \tag{41}$$

are satisfied, then, there exist positive constants ε^* and η^* such that for all $0 < \varepsilon < \varepsilon^*$, systems (39a) and (39b) have a unique exponentially stable periodic solution with the property

$$\left|\bar{Z}(t,\varepsilon) - Z_0^*\right| \le \eta^* \varepsilon, \tag{42}$$

with $Z_0^* = (0 \quad 0 \quad 0 \quad 0 \quad 0)^T$

See the proof of Theorem 4 in the appendix.

5. Simulation Results

The controlled system shown in Figure 1 is a single-phase series active power filter with half-bridge topology; its characteristics are placed in Table 2. The system under study augmented with the control system consisting of the grid observers (9a) and (9b) and control law (36) (see Figure 2) is simulated using MATLAB/SIMPOWER (V.R 2013a). The sensitive load is a bridge rectifier, supplying a resistor R in series with an inductor L. The controller implementation entails a proper choice of its design parameters. First, the gain vector components $K = (k_1 \quad k_2 \quad k_3)^T$, of the observer, are selected so that the conditions in equation (13) are satisfied. Second, the control performances depend on the numerical values given to the controller parameters, i.e., c_1 and c_2. The point is that there is no systematic way, especially in nonlinear control, to make adequate selection for these values. Therefore, the usual practice consists in proceeding with the trial-error approach starting from large initial values, e.g., in the interval $[10^3, 10^4]$ and tuning them, in one sense or the other, until a satisfactory behaviour is obtained. Doing so, the obtained values of observer and controller parameters are placed in Table 3.

5.1. Control Performances in the Presence of Grid Voltage Sags and considering the Constant Load. The objective of this simulation is to illustrate the behaviour of the proposed

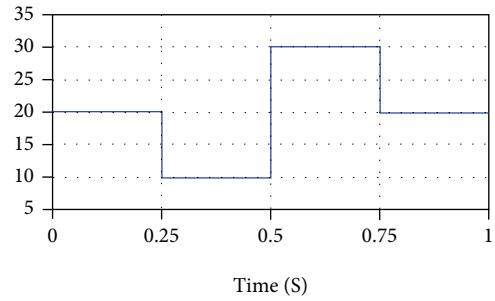

Figure 7: Load resistor changes.

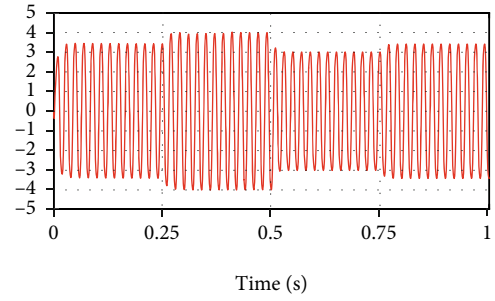

Figure 8: Load current i_L.

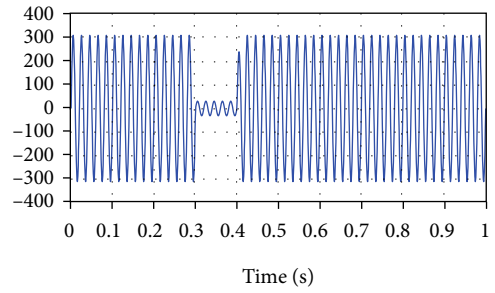

Figure 9: A sag in the grid voltage estimated $\widehat{x}_2$.

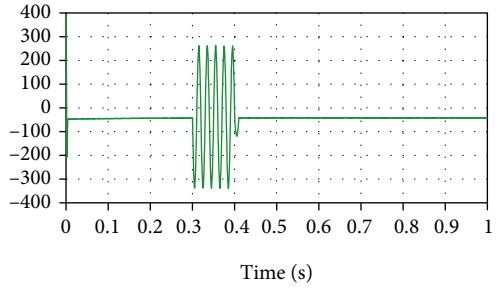

Figure 10: Compensation voltage v_s.

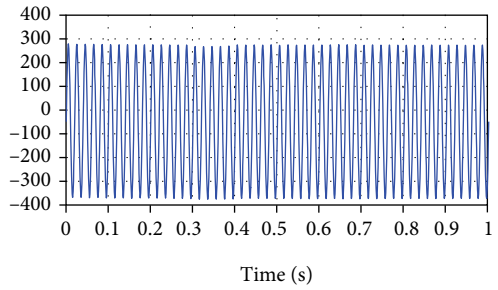

Figure 11: Voltage v_L at the terminals of sensitive load after compensation.

controller in the presence of the voltage sags in the single-phase power grid, while the load is kept constant ($R = 20\Omega$, $L = 500m\Omega$). The resulting controller performances are illustrated in Figures 3–6. Indeed, the performance of the grid observer, which is part of the proposed nonlinear controller, is illustrated in Figure 3(a), where the estimated signal, of the grid voltage $\widehat{x}_2$, provided by the grid observer converges rapidly to its true value v_n. A zoom is made in Figure 3(b) showing clearly the convergence of the proposed observer; this illustrates the efficiency of this grid observer. Figure 4 reveals a sag in the waveform of the estimated grid voltage $\widehat{x}_2$; the depth of which is 90% of the nominal voltage and of duration 100 ms, which exceeds the values fixed by the standard EN 50160. The compensation voltage v_s injected by the series active power filter is represented in Figure 5. To validate the performances of the proposed controller, Figure 6, for its part, shows that the voltage v_L, at the terminals of the sensitive load after compensation, is a sinusoidal signal; in this case, the voltage sag decreases sharply and its depth becomes 7% which is less than the value 10% imposed by the standard EN 50160. This confirms that the compensation of voltage sags is well achieved by the proposed controller.

5.2. Control Performances in the Presence of Grid Voltage Sags and considering Load Variations. The robustness of the proposed nonlinear control system is verified by taking into account variations in the load. Indeed, the simulation protocol is described in Figure 7 showing that the load resistance changes according to the following progression:

(i) A decrease of 50% at time 0.25 s

(ii) An increase of 50% at time 0.5 s

(iii) Return to its nominal value at the instant 0.75 s

Figures 8–10 illustrate the behaviour of the proposed nonlinear control system in the presence of grid voltage sag and by considering the load variations. In fact, Figure 8 shows the variation in the magnitude of the load current following the changes in the load resistance described in Figure 7. Figure 9 reveals a sag in the estimated signal of the grid voltage $\widehat{x}_2$; the depth of which is 90% of the nominal voltage and of duration 100 ms, which exceeds the values fixed by the 50160 standard. Figure 10 shows the compensation voltage v_s injected by the series active power filter. As for Figure 11, it shows that the voltage v_L at the terminals of the sensitive load after compensation is a sinusoidal signal; in this case, the voltage sag decreases sharply and its depth becomes 7% which is less than the value 10% imposed by the standard EN 50160. This confirms that the compensation of voltage sags is well achieved by the proposed controller.

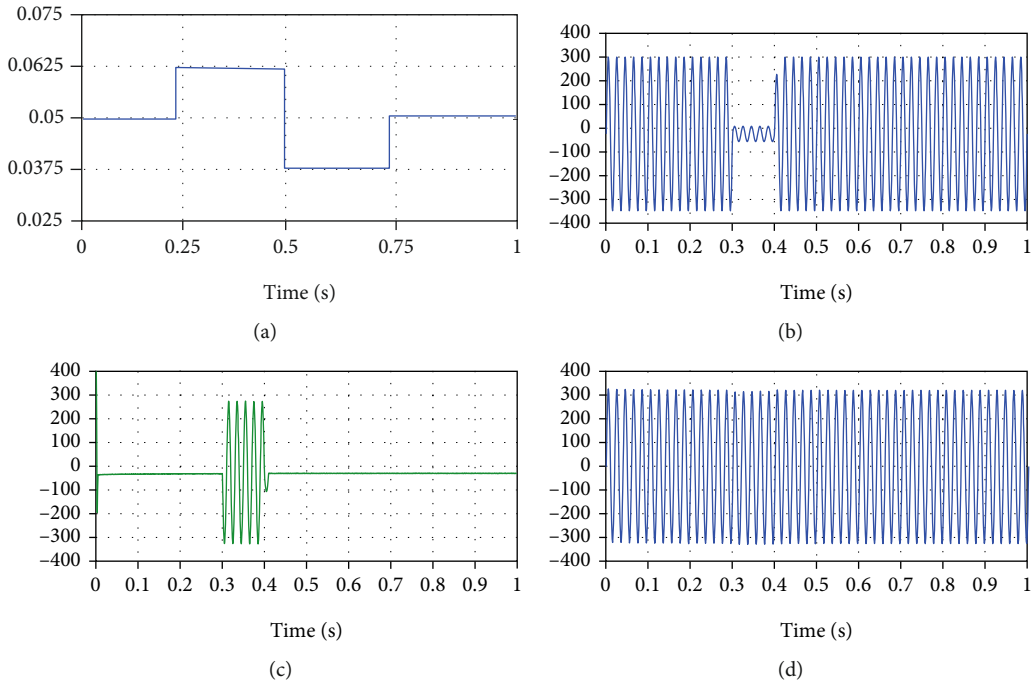

Figure 12: (a) Grid resistor changes. (b) A sag in the grid voltage estimated $\hat{x}_2$. (c) Compensation voltage v_s. (d) Voltage v_L at the terminals of the sensitive load after compensation.

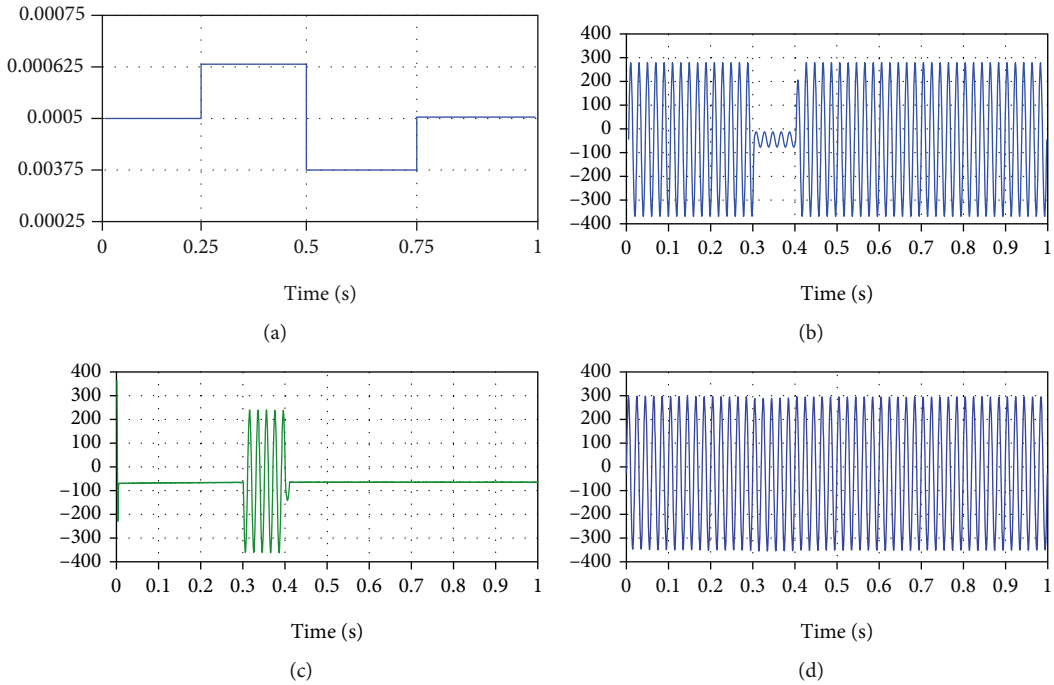

Figure 13: (a) Grid inductance changes. (b) A sag in the grid voltage estimated $\hat{x}_2$. (c) Compensation voltage v_s. (d) Voltage v_L at the terminals of the sensitive load after compensation.

In conclusion, this controller presents, in the presence of grid voltage sags and by considering the variations in load resistance, better tracking performance and greater robustness.

5.3. Control Performance Robustness to Grid Parameter Uncertainty. The robustness of the proposed nonlinear control system is now verified by considering parameter uncertainty on the grid impedance (R_n, L_n). Indeed, the

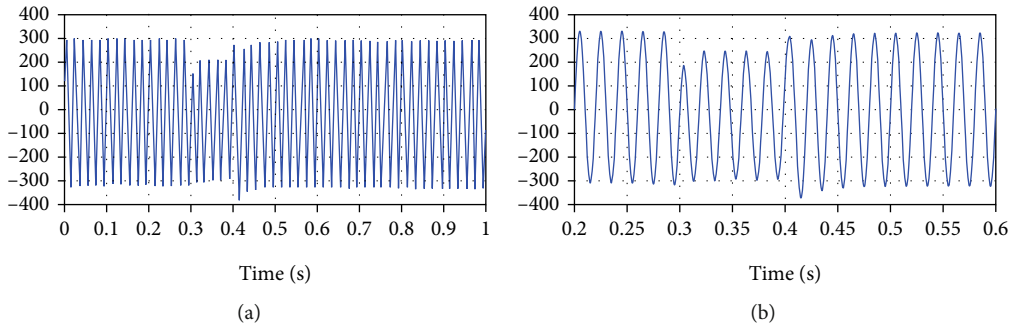

Figure 14: (a) Voltage v_L at the terminals of sensitive load after compensation; (b) zoom on this signal.

simulation protocol is described in Figures 12(a) and 13(a) showing that R_n and L_n are changed according to the following progression:

(i) An increase of 25% at time 0.25 s

(ii) A decrease of 25% at time 0.5 s

(iii) Return to its nominal value at time 0.75 s

It turns out that, vis-à-vis to the controller, the internal parameters of the grid (R_n and L_n) are subject to uncertainty on the interval [0.25 s; 0.75 s]. The latter will be referred to as uncertainty interval. All remaining system characteristics and controller parameters are kept unchanged with respect to Tables 2 and 3. The resulting control performances are illustrated in Figures 12(a)–12(d), in the case of resistor uncertainty, and Figures 13(a)–13(d), in the case of inductance uncertainty. It is seen that there is no deterioration of control performances despite the uncertainty of 25% on grid impedance (R_n, L_n). In particular, Figure 12(d) shows that the waveform sinusoidal, without sag, of the voltage v_L at the terminals of the sensitive load is always ensuring even with the uncertainty of the grid resistor.

It is observed in Figures 13(a)–13(d) that the uncertainty on the grid inductance L_n causes no performance deterioration of the controller. In particular, Figure 13(d) shows that the proposed controller ensures a sinusoidal voltage, without sag, at the terminals of the sensitive load during the interval of uncertainty.

5.4. Comparison with Linear Control. To highlight the better performances of the present nonlinear control, over the linear control strategy, a comparison is done, where a linear regulator of PID type is applied to the series active power filter under study. The parameters of the linear PID regulator are selected so that the regulation is satisfactory when the system operates in the nominal conditions corresponding to $E_n = 220\sqrt{2}$ V and $f_n = 50$ Hz.

The performances of the linear controller are illustrated in Figure 14 considering the same simulation scenario as described in Section 5.1 (see Figure 4).

Keep in mind that all parameters of the system under study cited in Table 2 are kept unchanged in this simulation. Figure 14(a) shows that the PID regulator performs well as long as the system remains operating in the nominal conditions, which is the case in the time interval [0 s, 0.3 s]. After this interval, the regulation performances deteriorate in the time interval [0.3 s, 0.4 s]. More specifically, Figure 14(b) shows that the peak value of load voltage v_L is much lower than its initial reference value of $220\sqrt{2}$ V (the depth of voltage sag is 40% and of duration 100 ms which exceeds the values fixed by the standard EN 50160). Consequently, this voltage sag in the voltage v_L causes the nonfunctioning of the sensitive load. The same Figure 14 shows that the sinusoidal shape with reference peak value $220\sqrt{2}$ V is preserved by the linear controller only in the time interval [0 s, 0.3 s]. In the time interval [0.4 s, 1 s], the waveform of v_L is sinusoidal but not symmetric. This clearly confirms that the performances of the linear controller are much less satisfactory, compared to those of the proposed nonlinear controller in which its performances are preserved throughout simulation time interval [0 s, 1 s] (see Figure 6).

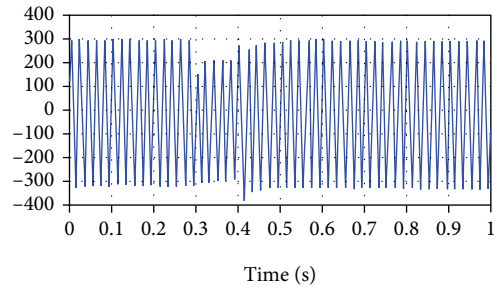

Figure 15: Voltage v_L at the terminals of sensitive load after compensation.

In the simulation, some comparisons with the SAPF system based on linear control are added to verify the effectiveness of the proposed SAPF control strategy by considering the same simulation protocol as described in Figure 7 (see Section 5.2) and the same simulation protocol as described in Figures 12(a) and 13(a) (see Section 5.3). Indeed, for the sake of comparison, Figure 11 shows that the sinusoidal shape of the load voltage v_L after compensation without sag is preserved throughout simulation time interval [0 s, 1 s] by the proposed nonlinear control, compared to the waveform observed in Figure 15 where the peak value of load voltage v_L is much lower than its initial reference value of $220\sqrt{2}$ V when using linear control (the depth of voltage

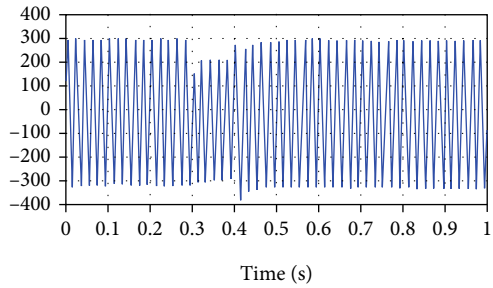

Figure 16: Voltage v_L at the terminals of sensitive load after compensation.

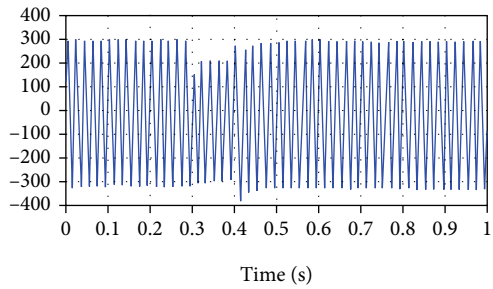

Figure 17: Voltage v_L at the terminals of sensitive load after compensation.

sag is 40% and of duration 100 ms which exceeds the values fixed by the standard EN 50160).

Also, Figures 12(d) and Figure 13(d) show that the sinusoidal shape of the load voltage v_L after compensation without sag is preserved throughout simulation time interval [0 s, 1 s] by the proposed nonlinear control, compared to the waveform observed in Figures 16 and 17 (the peak value of load voltage v_L is also much lower than its initial reference value of $220\sqrt{2}$ V when using linear control (the depth of voltage sag is 40% and of duration 100 ms which exceeds the values fixed by the standard EN 50160).

In Figures 15–17, it is obvious to discover that in the presence of grid voltage sags, the SAPF based on nonlinear control features better tracking performance at different simulation stages than the one based on linear control.

6. Conclusion

In this paper, we seek a control strategy for the single-phase series active power filter with half-bridge topology shown in Figure 1 to ensure the compensation of the grid voltage sags and subsequently protect the sensitive load. The considerable constraints of the control system of this filter are (i) the nonlinearity of the system dynamics, (ii) the high dimension of the system model, and (iii) the inaccessibility of some system variables to measurements. A nonlinear controller is proposed. It consists of the grid observer (10) and the control law (34) synthesized by using the Backstepping technique. A theoretical analysis, by using the Lyapunov stability and averaging theory, proves the achievement of the control objective. The simulation results show that the proposed controller meets its main control objective that is the compensation of voltage sags. The simulation results emphasize further the controller robustness to load changes and to grid parameter uncertainty. The simulation results also demonstrate the supremacy of the proposed nonlinear controller over a linear controller.

This study can be pursued in various directions, e.g., designing an efficient online grid voltage observer (in the presence of grid voltage harmonics).

Appendix

A. Stability Analysis

Proof. A. Part 1. Proposition 1 shows that the tracking errors $(e_1,\ e_2)$ in (37a) are globally asymptotically stable.

Part 2. Equations (39a) and (39b) are obtained from expressions (11), (30), and (35).

Part 3. The stability of the time-varying systems (39a) and (39b) is now analyzed by using the averaging theory [22, 23]. To this end, we introduce the following time-scale change: $\tau = \omega_n t$. It is easily checked from (39a) and (39b) that $W(\tau) = ^{def} Z(t) = Z(\tau/\omega_n)$ obeys the differential equation:

$$\dot{W}(\tau) = \varepsilon g(\tau, W, \varepsilon), \tag{A.1}$$

where

$$g(\tau, W, \varepsilon) = \begin{pmatrix} -c_1 w_1 + w_2 \\ -w_1 - c_2 w_2 \\ -\left(\dfrac{R_n}{L_n} + k_1\right) w_3 + \dfrac{w_4}{L_n} \\ -k_2 w_3 + w_5 \\ -k_3 w_3 - \omega_n^2 w_4 \end{pmatrix}. \tag{A.2}$$

From (A.2), the expression $g(\tau, W, \varepsilon)$ is a function of τ; it is 2π periodic. Now, let us introduce the averaged function:

$$g_0(W_0) \stackrel{def}{=} \lim_{\varepsilon \longrightarrow 0} \frac{1}{2\pi} \int_0^{2\pi} g(\tau, W_0, \varepsilon)\, d\tau, \quad W_0 \in \Re^5. \tag{A.3}$$

It readily follows from (A.2) that

$$g_0(W_0) = \begin{pmatrix} -c_1 w_{1,0} + w_{2,0} \\ -w_{1,0} - c_2 w_{2,0} \\ -\left(\dfrac{R_n}{L_n} + k_1\right) w_{3,0} + \dfrac{w_{4,0}}{L_n} \\ -k_2 w_{3,0} + w_{5,0} \\ -k_3 w_{3,0} - \omega_n^2 w_{4,0} \end{pmatrix}, \tag{A.4}$$

where $w_{i,0}$ $(i = 1, \cdots, 5)$ are the components of W_0. To obtain stability results about the system (A.1), it is enough (thanks to averaging theory) to analyze the following averaged system:

$$\dot{W}_0 = \varepsilon g_0(W_0). \tag{A.5}$$

Notice that, by considering equation (A.4), the time-invariant system (A.5) has a unique equilibrium at

$$W_0^* = (\,0 \quad 0 \quad 0 \quad 0 \quad 0\,)^T. \tag{A.6}$$

The stability of the equilibrium $W_0 = W_0^*$ of (A.5) will now be analyzed using the indirect Lyapunov method [22, 23]. As a result, we look if the Jacobian of the function $g_0(.)$, at $W_0 = W_0^*$, is Hurwitz. From (A.2), we obtain

$$A_r = \begin{pmatrix} A_1 & O \\ O & A_0 \end{pmatrix}, \tag{A.7}$$

where O are null matrices and the matrices A_1 and A_0 are as follows:

$$A_1 = \begin{pmatrix} -c_1 & 1 \\ -1 & -c_2 \end{pmatrix},$$
$$A_0 = \begin{pmatrix} -\left(\dfrac{R_n}{L_n} + k_1\right) & 1/L_n & 0 \\ -k_2 & 0 & 1 \\ -k_3 & -\omega_n^2 & 0 \end{pmatrix}. \tag{A.8}$$

The stability properties of the equilibrium W_0^* are fully determined by the state-matrix A_r. More specifically, the equilibrium W_0^* will be globally exponentially stable if the state matrix A_r is Hurwitz. Thus, it will be sufficient to verify that the state matrix A_r is Hurwitz. We have already noticed that the matrix A_0 is Hurwitz (see equation (11)). So, just check that matrix A_1 is also Hurwitz. To this end, note that the eigenvalues of matrix A_1 are the zeros of the following polynomial:

$$\det(\lambda I - A_1) = \lambda^2 + a_1\lambda + a_0. \tag{A.9}$$

Applying for example the well-known Routh's algebraic criteria, it follows that all zeros of the polynomial (A.9) have negative real parts if the conditions in (40) are satisfied. In other words, under these conditions, matrix A_r is Hurwitz. Then, by the indirect Lyapunov method, the equilibrium $W_0 = W_0^*$ of (A.5) is exponentially stable. Then, Part 3 follows from the averaging theory (e.g., [22], Theorem 10.4, and [23]). Theorem 4 is established. □

Data Availability

No data were used to support this study.

Conflicts of Interest

The authors declare that there is no conflict of interest regarding the publication of this paper.

References

[1] A. R. Nasrudin and I. Zeenat, "A single-phase series active power filter design," in *International Conference on Electrical, Electronic and Computer Engineering*, pp. 926–929, Cairo, Egypt, 2004.

[2] H. Ouadi, A. Aitchihab, and F. Giri, "Adaptive nonlinear control of three-phase series active power filters with magnetic saturation," *Journal of Control Automation and Electrical Systems*, vol. 31, no. 3, pp. 726–742, 2020.

[3] M. H. Antchev, M. Petkova, and V. T. Gurgulicov, "Sliding mode control of a single-phase series active power filter," in *EUROCON, The International Conference on Computer as a Tool*, pp. 1344–1349, Warsaw, Poland, 2007.

[4] Y. Abouelmahjoub, S. El Beid, H. Abouobaida, and A. Chellakhi, "Advanced nonlinear control of single phase half bridge series active power filter," in *2020 IEEE 2nd International Conference on Electronics, Control, Optimization and Computer Science (ICECOCS)*, Kenitra, Morocco, 2020.

[5] N. Karthik and M. S. Kalavathi, "Simulation and experimental implementation of single phase active power filters for improving power quality," *International Journal of Applied Engineering Research*, vol. 13, pp. 9137–9144, 2018.

[6] L. F. J. Meloni, F. L. Tofoli, Â. J. J. Rezek, and E. R. Ribeiro, "Modeling and experimental validation of a single-phase series active power filter for harmonic voltage reduction," *IEEE Access*, vol. 7, pp. 151971–151984, 2019.

[7] N. F. Teixeira, J. G. O. Pinto, M. J. S. Freitas, and J. L. Afonso, "New control algorithm for single-phase series active power filter," *Electric Power Components and Systems*, vol. 7, pp. 1752–1760, 2015.

[8] J. L. Torre, L. A. M. Barros, J. L. Afonso, and J. G. Pinto, "Development of a proposed single-phase series active power filter without external power sources," in *International Conference on Smart Energy Systems and Technologies*, pp. 1–6, Porto, Portugal, 2019.

[9] E. R. Ribeiro and I. Barbi, *A Series Active Power Filter for Harmonic Voltage Suppression*, INTELEC, Edingurgh, U.K., 2001.

[10] G. Zhu, G. Wang, and D. Hua, "Sliding mode control with variable structure of series active power filter," in *2009 IEEE Power & Energy Society General Meeting*, pp. 1–6, Calgary, AB, Canada, 2009.

[11] B. Benazza and H. Ouadi, "Backstepping control of three-phase multilevel series active power filter," in *2020 International Conference on Electrical and Information Technologies (ICEIT),*, pp. 1–6, Rabat, Morocco, 2020.

[12] S. Ramirez, N. Visairo, M. Oliver, C. Nuñez, V. Cárdenas, and H. Sira-Ramirez, "Harmonic compensation in the AC mains by the use of current and voltage active filters controlled by a passivity-based law," in *7th IEEE International Power Electronics Congress. Technical Proceedings. CIEP 2000 (Cat. No. 00TH8529)*, pp. 87–92, Acapulco, Mexico, 2000.

[13] M. I. Marei, E. F. El-Saadany, and M. M. A. Salama, "An efficient control of the series compensator for sag mitigation and voltage regulation," in *IEEE 34th Annual Conference on Power Electronics Specialist, 2003. PESC'03*, pp. 1242–1247, Acapulco, Mexico, 2003.

[14] I. Annapoorani, R. Samikannu, and K. Senthilnathan, "Series active power filter for power quality improvement based on distributed generation," *International Journal of Applied Engineering Research*, vol. 12, pp. 12214–12218, 2017.

[15] S. W. Han, S. Y. Lee, and G. H. Choe, "A 3-phase series active power filter with compensate voltage drop and voltage unbalance," *IEEE International Symposium on Industrial Electronics Proceedings*, vol. 2, pp. 1032–1037, 2020.

[16] C. K. Tse and M. H. L. Chow, "Theoretical study of switching power converters with power factor correction and output regulation," *IEEE Transactions on Circuits and Systems*, vol. 47, no. 7, pp. 1047–1055, 2000.

[17] A. Abouloifa, F. Giri, I. Lachkar, and F. Z. Chaoui, "Formal framework for nonlinear control of PWM AC/DC boost rectifiers controller design and average performance analysis," *IEEE Transactions on Control Systems Technology*, vol. 18, no. 2, pp. 323–335, 2010.

[18] I. Lachkar, F. Giri, A. Abouloifa et al., "Nonlinear control of single-phase shunt active power filter theoretical analysis of closed-loop performances," *IFAC Proceedings Volumes*, vol. 44, pp. 4954–4959, 2011.

[19] E. Samadaei, M. Iranian, M. Rezanejad, R. Godina, and E. Pouresmaeil, "Single-phase active power harmonics filter by op-amp circuits and power electronics devices," *Sustainability Journal*, vol. 10, no. 12, pp. 4406–4413, 2018.

[20] H. Hammouri, G. Bornard, and K. Busawon, "High gain observer for structured multi-output nonlinear systems," *IEEE Transactions on Automatic Control*, vol. 55, no. 4, pp. 987–992, 2010.

[21] M. Krstic, I. Kanellakopoulos, and P. V. Kokotovic, *Nonlinear and Adaptive Control Design*, John Willy & Sons, New York, 1995.

[22] H. Khalil, *Nonlinear Systems (3th Ed)*, Prentice-Hall, Upper Saddle River, New Jersey, 2002.

[23] Y. Abouelmahjoub, A. Abouloifa, F. Z. Chaoui, F. Giri, and M. Kissaoui, "Observation and nonlinear control of single phase half bridge shunt active power filter," in *IEEE International Conference on Multimedia Computing and Systems (ICMCS'14)*, Marrakech, Morocco, 2014.